Research Article | Vol. 25, No. 4 | 20 Feb 2017 | OPTICS EXPRESS 4393

Optics EXPRESS

# Highly sensitive miniature fluidic flowmeter based on an FBG heated by $Co^{2+}$-doped fiber

ZHENGYONG LIU,[1,*] LIN HTEIN,[1] LUN-KAI CHENG,[2] QUINCY MARTINA,[2] ROB JANSEN,[2] AND HWA-YAW TAM[1]

[1]*Photonics Research Center, Department of Electrical Engineering, The Hong Kong Polytechnic University, Hung Hom, Kowloon, Hong Kong, China*
[2]*TNO, Stieltjesweg 1, 2628 CK Delft, Netherlands*
[*]*zhengyong.liu@connect.polyu.hk*

**Abstract:** In this paper, we present a miniature fluidic flow sensor based on a short fiber Bragg grating inscribed in a single mode fiber and heated by $Co^{2+}$-doped multimode fibers. The proposed flow sensor was employed to measure the flow rates of oil and water, showing good sensitivity of 0.339 nm/(m/s) and 0.578 nm/(m/s) for water and oil, flowing at $v$ = 0.2 m/s. The sensitivity can be increased with higher laser power launched to the $Co^{2+}$-doped multimode fibers. A small flow rate of 0.005 m/s and 0.002 m/s can be distinguished for a particular phase of water or oil, respectively, at a certain laser power (i.e. ~1.43W). The flow sensor can measure volume speed up to 30 L/min, which is limited by the test rig. The experimental results show that the sensor can discriminate slight variation of flow rates as small as 0.002m/s.



**OCIS codes:** (280.0280) Remote sensing and sensors; (060.3735) Fiber Bragg gratings; (280.2490) Flow diagnostics.

## References and links

1. A. D. Kersey, M. A. Davis, H. J. Patrick, M. LeBlanc, K. P. Koo, C. G. Askins, M. A. Putnam, and E. J. Friebele, "Fiber grating sensors," J. Lightwave Technol. **15**(8), 1442–1463 (1997).
2. H. H. Bruun, *Hot-Wire Anemometry: Principles and Signal Analysis* (Oxford University, 1995).
3. V. T. Morgan, "The Overall Convective Heat Transfer from Smooth Circular Cylinders," Adv. Heat Transf. **11**, 199–264 (1975).
4. Y. H. Wang, C. P. Chen, C. M. Chang, C. P. Lin, C. H. Lin, L. M. Fu, and C. Y. Lee, "MEMS-based gas flow sensors," Microfluid. Nanofluidics **6**(3), 333–346 (2009).
5. S. Gao, A. P. Zhang, H.-Y. Tam, L. H. Cho, and C. Lu, "All-optical fiber anemometer based on laser heated fiber Bragg gratings," Opt. Express **19**(11), 10124–10130 (2011).
6. K. P. Chen, B. McMillen, M. Buric, C. Jewart, and W. Xu, "Self-heated fiber Bragg grating sensors," Appl. Phys. Lett. **86**(14), 143502 (2005).
7. J. Cheng, W. Zhu, Z. Huang, and P. Hu, "Experimental and simulation study on thermal gas flowmeter based on fiber Bragg grating coated with silver film," Sens. Actuators A Phys. **228**, 23–27 (2015).
8. Z. Liu, M. L. Tse, A. P. Zhang, and H. Y. Tam, "Integrated microfluidic flowmeter based on a micro-FBG inscribed in $Co^{2+}$-doped optical fiber," Opt. Lett. **39**(20), 5877–5880 (2014).
9. Y. Li, G. Yan, L. Zhang, and S. He, "Microfluidic flowmeter based on micro "hot-wire" sandwiched Fabry-Perot interferometer," Opt. Express **23**(7), 9483–9493 (2015).
10. X. Wang, X. Dong, Y. Zhou, K. Ni, J. Cheng, and Z. Chen, "Hot-wire anemometer based on silver-coated fiber Bragg grating assisted by no-core fiber," IEEE Photonics Technol. Lett. **25**(24), 2458–2461 (2013).
11. L. J. Cashdollar and K. P. Chen, "Fiber Bragg grating flow sensors powered by in-fiber light," IEEE Sens. J. **5**(6), 1327–1331 (2005).
12. P. Caldas, P. A. S. Jorge, G. Rego, O. Frazão, J. L. Santos, L. A. Ferreira, and F. Araújo, "Fiber optic hot-wire flowmeter based on a metallic coated hybrid long period grating/fiber Bragg grating structure," Appl. Opt. **50**(17), 2738–2743 (2011).
13. S. Takashima, H. Asanuma, and H. Niitsuma, "A water flowmeter using dual fiber Bragg grating sensors and cross-correlation technique," Sens. Actuators A Phys. **116**(1), 66–74 (2004).
14. J. T. W. Kuo, L. Yu, and E. Meng, "Micromachined Thermal Flow Sensors—A Review," Micromachines (Basel) **3**(4), 550–573 (2012).
15. M. Melani, L. Bertini, M. De Marinis, P. Lange, F. D'Ascoli, and L. Fanucci, "Hot wire anemometric MEMS sensor for water flow monitoring," Proc. –Design. Autom. Test Eur. 342–347 (2008).
16. R. Ahrens and K. Schlote-Holubek, "A micro flow sensor from a polymer for gases and liquids," J. Micromech. Microeng. **19**(7), 074006 (2009).

#283278 https://doi.org/10.1364/OE.25.004393
Journal © 2017 Received 5 Jan 2017; revised 29 Jan 2017; accepted 1 Feb 2017; published 16 Feb 2017

Optics EXPRESS

17. R. Ahrens and M. Festa, "Dynamical flow measurements in hydraulic systems using a polymer-based micro flow sensor," Procedia Chem. **1**(1), 927–930 (2009).

## 1. Introduction

Precise measurement of fluid flow rate attracts a lot of attention due to the applicable demands in oil industry where there is the need to develop miniature sensors for downhole so that the flow rate of oil/water can be monitored in real time, to determine the volume of the exploration oil. In the past two decades, fiber Bragg gratings (FBGs) have been developed into various types of fiber-optic sensors with very good performance in terms of accuracy, fast response, EM immunity and simple interrogation [1]. Because signal propagating in optical fiber exhibits low loss, long-distance sensing is possible by using fiber-optic sensing technique in oil industry. Hot-wire anemometer (HWA) is a well-known technique for wind speed measurement, where an electrical wire / film is heated up by an electric current and the speed of wind flow around the HWA is determined by the cooling rate of the wire/film [2–4]. Similar approach is adopted by using light absorption fibers, *e.g.* $Co^{2+}$-doped fiber [5], or metal-film coated fiber [6,7]. The cobalt doped inside fiber core in [5] or coating of metal film (*e.g.* silver) on the outside of fiber [6,7] converts optical power to heat. Not only wind flow speed but also microfluidic water flow rate can be precisely measured by using an FBG written in the light absorption fibers [8,9]. Very small change of microfluidic flow rate of ~16 nL/s was detected by integrating FBG in $Co^{2+}$-doped fiber [8]. Using metal-film coated on the outside of the cladding as the heating element is less effective compared to the cobalt-doped fiber approach where the heating element is located in the fiber core. Furthermore, the metal-film approach requires the coupling of laser light from the core to the cladding so that light can be absorbed by the metal film to generate heat, for example, by using no-core fiber [10], multimode fiber [11], optical tab [6], LPG [12] and core-offset splice [7]. In the metal film technique, the optical-to-heat efficiency is highly dependent on the type of metal, the coated length of metal film and the light expanding components. Most hot-fiber sensors are designed for anemometer to measure wind speed, where the fiber can be heated to reach high temperature under low laser power as the air has relatively low heat capacity.

To measure hot fluidic flow, such as water and oil, high energy conversion efficiency from light to heat is desirable. Several approaches have been proposed to measure water flow speed. In 2005, Takashima *et al* [13] proposed the use of dual-FBG sensors to detect the time delay of vortex signal generated by a bluff body before FBG sensors, so that the flow rate could be determined from the cross-correlation of two sensors. A minimum detectable velocity of 0.05 m/s was achieved. In microfluidics, the technique of micro-electro-mechanical-systems (MEMS) has been used to measure the microfluidic flow rate with configurations of hot-wire, hot-film and calorimetry [14,15]. The measurement range can be up to 2.5 m/s with a repeatability of ± 1% [15]. However, due to the micro electrical-wires/films used, the volume speed of the fluid cannot be too large, typically less than 1 L/min [14,16]. To measure hydraulic oil in large volume, Ahrens *et al* proposed to use a polymer-based microflow meter containing electrical heaters and thermometers. The fluid flow rate was measured up to 80 L/min [17]. However, electrical based sensors show poor performance in harsh environment such as strong electromagnetic interference.

In this paper, we present a simple and compact fluid flowmeter based on FBG heated by $Co^{2+}$-doped multimode fiber, which can measure flow rate of water and hydraulic oil with good performance in terms of sensitivity for volume velocity measurement. To the best of our knowledge, this is the first time miniature FBG-based HWA is used successfully to measure oil flow rate in large volume, which could be of great interest to the oil industry. The sensor head can be heated up to high temperature by several $Co^{2+}$-doped multimode fibers which are pumped with light from semiconductor diode lasers located at one end of the fibers through commercial MMFs. In a zero-flow experiment, the temperature of the FBG in the sensor head can reach over 200 °C – while the oil temperature is maintained at 130°C, demonstrating that

Optics EXPRESS

the sensor could be used to measure flow rate of hot fluid. The flow rate measurement experiments were conducted at a test rig at TNO in the Netherland. The test rig was designed for flow-rate measurement of air, water, and oil but has no provision to heat fluid.

## 2. Characterization of the fluid flow sensor

Figure 1 shows the schematic figure of the proposed sensor used to measure flow rate of fluid, (i.e. water and oil). To fabricate the flowmeter, a 3-mm long FBG was inscribed in a standard single mode fiber (SMF28). Short FBG is utilized so as to minimize the chirp effect when the grating is heated. Then, a short $Co^{2+}$-doped multimode fiber (MMF) with 50μm core and 125μm cladding is spliced to a commercial multimode fiber, which has the same core and cladding size. The two MMFs have the same NA of 0.2, so that the splicing loss can be minimized. The length of the $Co^{2+}$-doped MMF is cleaved to ~5 mm. The sensor consists of the single mode fiber with the FBG surrounded by 4 identical $Co^{2+}$ doped MMFs. All 5 fibers were inserted into a stainless steel tube which has an inner and outer diameter of 380 μm and 500 μm, respectively. The small size of the tube used can weaken the vortex effect caused by the sensor itself, which may result in temperature fluctuation especially when the flow is fast. The FBG and $Co^{2+}$-doped MMFs are located at the same position along the stainless steel tube, as shown in Fig. 1. The four 5-mm long $Co^{2+}$-doped MMFs can be heated by launching laser light to the commercial MMFs which are spliced to the $Co^{2+}$-doped MMFs. All five fibers are packaged and protected by the stainless steel tube. The ideal cross-sectional view of the sensor head is also shown in the inset, where the FBG to be heated is surrounded by the four $Co^{2+}$-doped fibers. The gaps between fibers are filled with heat sink to transfer the heat uniformly and fix the fibers spatially. The lengths of $Co^{2+}$-doped fibers and FBG are controlled precisely during stacking, which guarantees that no misalignment exists at sensor head. The length of steel tube used for protection is 10 cm, which however is depending on the pipe size and can be shortened to fit small size of pipe as the sensor head is only 5 mm long. Note that isopropyl alcohol (IPA) is filled in steel tube before stacking to eliminate static electricity and pumped out later, so as to minimize the mechanical strain transferred to the sensing FBG to avoid strain-induced wavelength shift. After stacking, the glue is filled at both ends of the tube to fix all the fibers spatially.

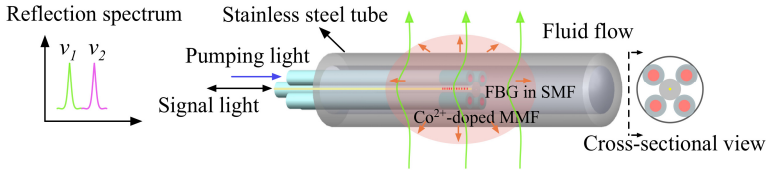


Fig. 1. Schematic figure of the fluid flow sensor.

To characterize the temperature response of the flow sensor, a calibration setup was used. The flow sensor was placed in hot water close to but less than 100°C. The Bragg wavelength was monitored when the water was cooled down. For comparison, a bare FBG written on the same single mode fiber as the flow sensor was placed close to the sensing head. The results are plotted in Fig. 2(a). It can be seen that the temperature dependence of both gratings is ~10.7 pm/°C, although the flow sensor is packaged inside the stainless steel tube. Using this calibration value, one can calculate the exact temperature of the heated FBG by detecting the Bragg wavelength change, *i.e.* 10.7 pm shift equals to one degree Celsius. The effect of laser heating was tested by putting the flow sensor in water at room temperature, hot water at <100 °C and hot oil at ~130 °C. The output power of the 976 nm laser was increased gradually. Figure 2(b) shows the wavelength shifts with respect to different pump powers. Even though at different fluidic conditions, the laser heating process follows a linear relationship, which is also similar to other flow sensors based on hot-fibers [6,8,9]. Another important parameter that affects the measurement result is the different heating efficiency of water and oil. The

Optics EXPRESS

heat capacity of oil (~1.88 $J \cdot g^{-1} \cdot K^{-1}$) is lower than that of water (4.18 $J \cdot g^{-1} \cdot K^{-1}$), and therefore for the same amount of laser power, higher temperature was recorded in the flow sensor which was placed in oil. This is also in good agreement with the electrical micro flow sensor based on thermal anemometric principle [16]. When the sensor was immersed in hot water, the grating needs slightly more laser power to heat it up to attain the same temperature difference than when the sensor was immersed in cold water. The reason is that the heat capacity of hot water close to 100 °C, i.e. 4.219 $J \cdot g^{-1} \cdot K^{-1}$, is slightly larger than that at room temperature. This indicates that in measuring hot fluid flow, more laser power is needed to obtain large temperature difference between the fluid and the sensor head, especially for fluids with large heat capacity. The inset of Fig. 2(b) shows the spectrum shift of the FBG when heated inside the hydraulic oil. Owing to the short grating length used, no chirp effect was observed even though at high temperature of hundreds of degrees.

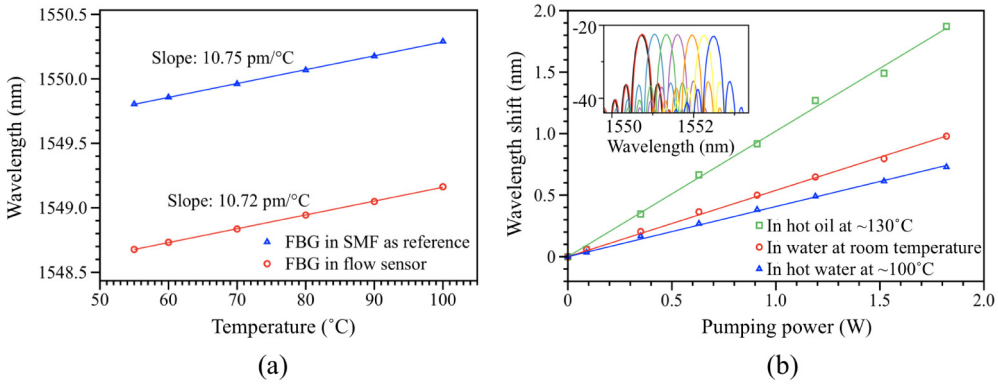


Fig. 2. (a) Temperature response of the flow sensor and (b) wavelength shifts of the flow sensor placed in water at room temperature and ~100°C, and hot oil at ~130°C when pumped by 980 laser with increasing power, the inset shows the spectrum shift of FBG in the hot oil.

As there are multiple $Co^{2+}$-doped multimode fibers packaged adjacent to the FBG, more than one $Co^{2+}$-doped fiber can be used to heat the grating, especially in fluid with larger heat capacity and hence more heating power is needed. We demonstrated experimentally the capability of multiple-pumping the flow sensor by launching two 976 nm lasers into two of the four $Co^{2+}$-doped fibers. The Bragg wavelength shift is plotted in Fig. 3 when the two lasers were turned on and off, which are set at the same output power level. About ~0.73 nm wavelength shift was obtained by pumping only one laser, and extra shift of ~0.77 nm was achieved when the second pumping laser was switched on. After turning off the second laser, the peak wavelength of the grating returned to its previous value, indicating that the performance of the flow sensor is repeatable and stable. The multiple pumping scheme of the proposed flow sensor is very advantageous for applications requiring large temperature difference to measure large flow speed or for fluids with large heat capacity.

Optics EXPRESS

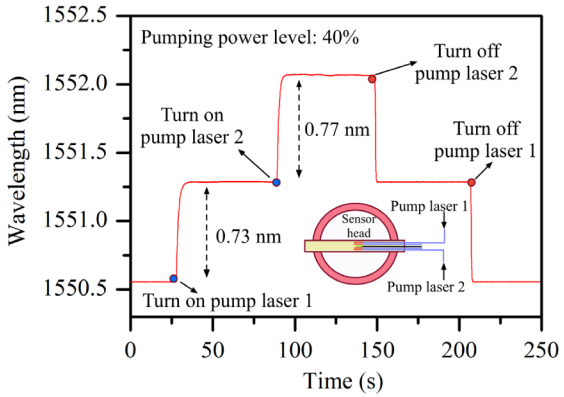


Fig. 3. Demonstration of the temperature increase of the flow sensor when pumped at one laser only and two lasers simultaneously.

## 3. Flow measurement

To measure the fluidic flow rate, the sensor needs to be heated to a constant temperature by launching sufficient laser light to the $Co^{2+}$-doped fiber. When there is no fluidic flow, the sensor and the fluids will be at an equilibrium convection state. Once the flow starts, the fluids carry away the heat from the sensor. Based on the principle of "hot-wire anemometer (HWA)", the heat loss, $H_{loss}$, can be expressed in term of the flow rate, $v$, as below [2]

$$H_{loss} = (A + B \cdot \sqrt{v}) \cdot \Delta T, \tag{1}$$

where $\Delta T$ is the temperature change of the sensor, $A$ and $B$ are empirical constants for the fluid, which can be determined by calibration. Since the FBG is used to measure the temperature change, the wavelength shift, $\Delta\lambda$, of the FBG with temperature can be expressed by [1]

$$\Delta\lambda = 2n_{eff}\Lambda\left(\alpha + \frac{1}{n_{eff}}\frac{dn_{eff}}{dT}\right)\Delta T, \tag{2}$$

where $n_{eff}$ is the effective index of the fundamental mode of the fiber, $\alpha$, $\Lambda$ is the coefficient of thermal expansion and grating pitch. By substituting Eq. (1) in Eq. (2), one can deduce the relationship between the Bragg wavelength and the flow rate as follows

$$\lambda = \lambda_0 + 2n_{eff}\Lambda\left(\alpha + \frac{1}{n_{eff}}\frac{dn_{eff}}{dT}\right)\frac{H_{loss}}{A + B \cdot \sqrt{v}}. \tag{3}$$

At a certain laser power, the curve of the Bragg wavelength and the fluidic flow rate is determined by Eq. (3), which can be utilized to monitor the flow rate by detecting the Bragg wavelength change of FBG.

### *3.1 Flow measurement*

In the experiment, water and hydraulic oil were used to conduct the flow measurement. In the measurement setup of the fluidic flow rate shown in Fig. 4, the stainless steel tube of the flow sensor was inserted perpendicularly into a Plexiglas tube with inner diameter of 25 mm, where the sensor head was placed in the center of the tube to measure the flow rate. A 976-nm semiconductor laser with 50/125-μm multimode fiber pigtail was connected to one of the four $Co^{2+}$-doped MMFs to heat the grating. As the water and oil flow was measured at room temperature due to the rest rig, the initial temperature difference is enough by pumping one $Co^{2+}$-doped fiber. Even so, the multiple-pumping scheme, as demonstrated in Fig. 3, can be

Optics EXPRESS

used to increase the temperature difference larger for extreme fluidic condition such as hot fluids. Due to the small size of the sensor, the heating asymmetry can be ignored when one or more $Co^{2+}$-doped are pumped. The FBG with single mode fiber pigtail was connected to an interrogator (SM130) to monitor the FBG wavelength to obtain the temperature of the FBG.

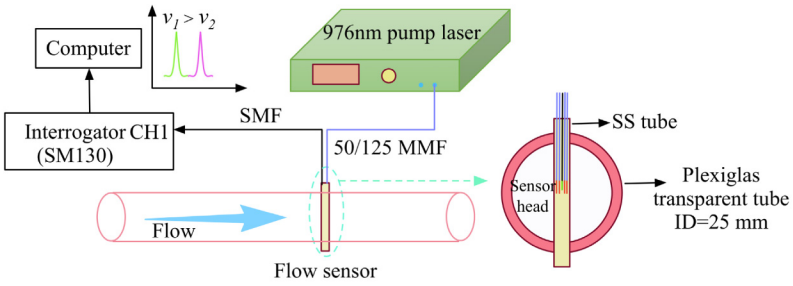


Fig. 4. Schematic setup use to measure the water and oil flow rate.

The entire test rig, shown in Fig. 5(a), is located at TNO, The Netherlands, which has a complete flow controlling system of oil and water. Large tanks are used to guarantee enough fluid volume at high flow rate. Figures 5(b)-5(d) show the photos of the Plexiglas tube when no fluid, water, and hydraulic oil were passing through, respectively. At different laser power level of 100%, 80%, 60%, 40%, 20%, corresponding to actual optical power of 1.962 W, 1.799 W, 1.431 W, 0.961 W, and 0.557 W, the Bragg wavelength of the FBG was monitored and logged at a frequency of 100 Hz for different flow rates. Table 1 lists all the settings of the flow rates for water and oil. The flow rate of the test rig was precisely controlled with conventional flow sensors in the flow systems.

**Table 1. Settings of the flow rates for oil and water during the measurement, $\rho_{water}$ = 1000 kg/m$^3$, $\rho_{oil}$ = 878 kg/m$^3$.**

| Mass flow rate (kg/hr) | 0 | 50 | 100 | 200 | 400 | 600 | 800 | 1750 |
|---|---|---|---|---|---|---|---|---|
| Water flow rate (m/s) | 0 | 0.028 | 0.057 | 0.113 | 0.226 | 0.34 | 0.453 | 0.99 |
| Oil flow rate (m/s) | 0 | 0.032 | 0.064 | 0.129 | 0.258 | 0.387 | 0.516 | — |

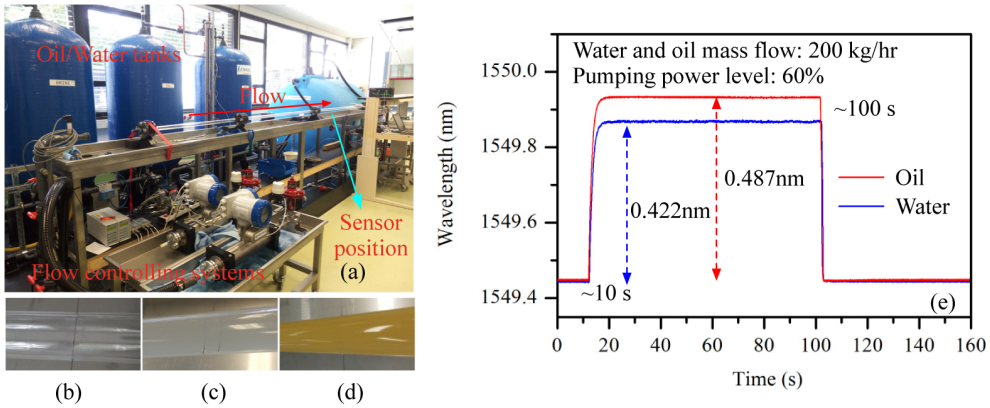


Fig. 5. Photos of the (a) test rig and the Plexiglas tube when (b) no fluid (c) water and (c) hydraulic oil are flowing inside respectively. (e) Wavelength shifts of the FBG when oil and water are flowing individually at the same mass flow rate of 200 kg/hr and pumping power level of 60%.

During the measurement, after logging the Bragg wavelength for ~10 s, the laser was switched on. The laser was switched on for ~90 s to reach equilibrium of the heat convection, and then switched off. As it can be observed from the results shown in Fig. 5(e), where the mass flow rate of the water and oil is 200 kg/hr, the Bragg wavelength of the FBG stays quite

Optics EXPRESS

stable whether there is flow or not. Because of the different heat capacity of the fluids, the total wavelength shift (0.487 nm) of oil is higher than that (0.422 nm) of water, which means that at the same flow rate, oil carried less heat than water. When the laser was switched off, the sensor was cooled down very quickly (within ~1 s), which includes the response time of the laser itself.

Figure 6 plots the wavelength shift at different flow rates, where Figs. 6(a) and 6(b) are the results for water flow, and Figs. 6(c) and 6(d) are the results for the oil flow. Figures 6(a) and 6(c) show the wavelength changes for the mass flow speed of 100 kg/hr and 800 kg/hr for water and oil, respectively, at different laser power levels. The Bragg wavelength shift can be clearly seen at the two flow rates and larger wavelength shift is obtained for the oil flow. Figures 6(b) and 6(d) show the wavelength shift of the sensor at different flow rates of water and oil, respectively, at laser power level of 60%. There is a large shift between no flow and very small flowing rate because no heat was taken away if the fluid stays static. These experiments demonstrated that the sensor successfully measured the flow rate of oil and water at room temperature. Flow rate of hot water and hot oil could also be measured. Figure 2(b) shows that sufficiently large temperature difference can be achieved between the sensor and 100°C water or between the sensor and 130°C oil. Furthermore, larger temperature difference can be easily attained using lasers with higher power or with multiple-laser configuration for measuring flow rate of hot fluids at higher temperature.

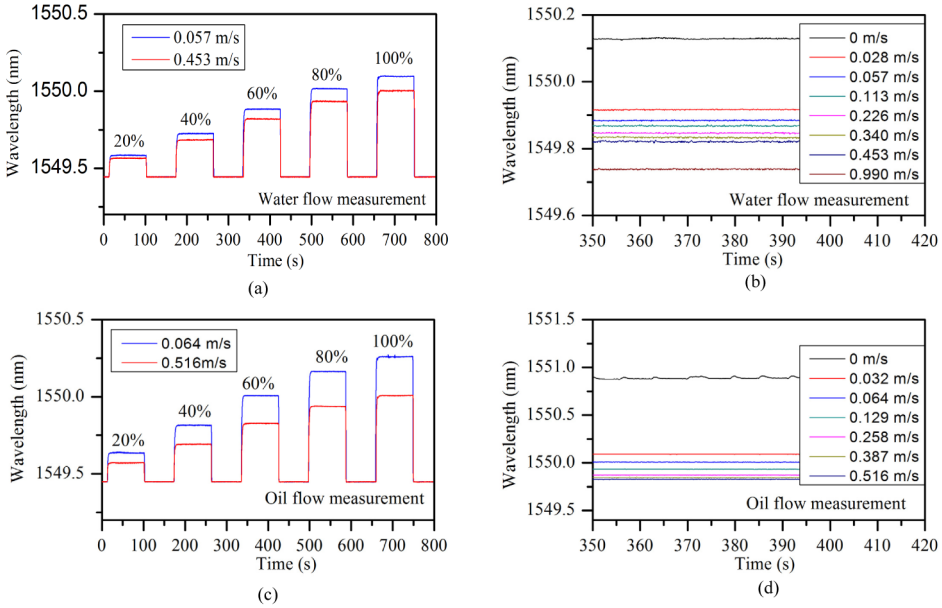


Fig. 6. Bragg wavelength shift of (a) water and (c) oil flow measurement for two different flow rates at the pumping power level of 20%, 40%, 60%, 80% and 100%, (b) and (d) show the wavelength shift at the pumping power level of 60% for all the measured flow rates, respectively

### *3.2 Sensitivity*

The sensitivity of the flow sensor was determined by plotting the wavelength shifts as a function of the flow rate for the pump power levels of 100% to 20%, as illustrated in Fig. 7. The experimental data for different pump power levels were fitted via Eq. (3). A fitting $R^2$ value of ~0.999 is found for the oil flow. It is worth indicating that for the water flow, the fitting $R^2$ is larger than 0.99, which can be acceptable, except for the case of 100%. Because of this, the measured data of 60% is chosen as the sensor characterization. By studying the first derivative of the fitted data, the sensitivity with respect to the flow rates can be obtained

Optics EXPRESS

and shown in Figs. 7(b) and 7(d) for water and oil flow. At lower flow rate, the sensitivity is much higher than that at large rate region. This is because of the nonlinear convection process according to the thermal anemometric principle, which is described by Eq. (3). Taking the flow rate of 0.2 m/s as an example, the flow sensitivities at the pumping power level from 20% to 100% are 0.066 nm/(m/s), 0.135 nm/(m/s), 0.220 nm/(m/s), 0.288 nm/(m/s), 0.339 nm/(m/s) for the water flow, and 0.146 nm/(m/s), 0.276 nm/(m/s), 0.409 nm/(m/s), 0.509 nm/(m/s), 0.578 nm/(m/s) for the oil flow. It can be seen that higher pump power leads to better sensitivity. Also, at the same flow setting and pump power, the flow sensor has higher sensitivity to measure the oil flow than water. This can be explained by the lower heat capacity of oil that causes higher temperature difference inside the oil flow than water flow when the $Co^{2+}$-doped fiber converts the same amount of optical power to heat. In particular, at the same pump power of 100% (~1.96 W), the temperature difference obtained inside the oil without flow was as high as ~200 °C, much higher than that inside the water, which is ~100 °C. It is noted that the viscosity and pressure of the fluids, which are temperature dependent, show negative effect on the sensitivity as the heat on FBG is taken away slowly. The heat capacity of the fluids with various viscosities (e.g. water and oil) is different, which will influence the heating efficiency as demonstrated in Fig. 2(b). Therefore, single phase of water / oil is investigated individually in the experiments so that the viscosity is constant. The study of the viscosity effect will be carried on by mixing water and oil in future work.

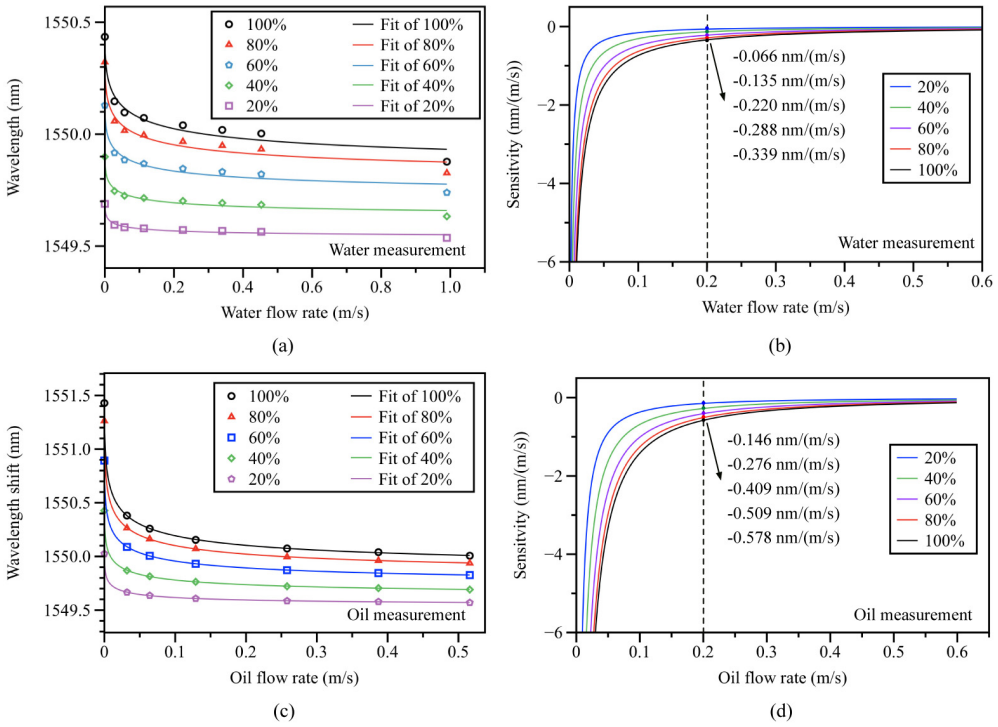


Fig. 7. Bragg wavelength shifts as a function of (a) water flow rate and (c) oil flow rate at different pump power levels, (b) and (d) are the sensitivities with respect to the flow rates of both measurands respectively.

In the experiment, the maximum flow rate is limited by the fluid amount of the test rig, which is ~1 m/s for water and ~0.5 m/s for oil. Nevertheless, the volume flow velocity of water can reach ~30 L/min, which is larger than the reported liquid flow sensors based on hot-wire/film [14,16]. It is possible to measure even larger mass flow and higher flow rate by increasing the heat generation by pumping multiple $Co^{2+}$-doped fibers. Figure 8 shows the

Optics EXPRESS

sensitivity of oil and water flow measurement at the rate of 0.2 m/s with respect to different pump power. As expected, the sensitivity can be improved simply by increasing the laser power. The increase also follows a linear relationship, which is similar to the hot-fiber anemometer [5]. To achieve similar sensitivity in flow rate, water with higher heat capacity needs more laser power than oil. Based on the sensitivity at $v$ = 0.2 m/s region and the resolution of the standard interrogator used, *i.e.* 1 pm, theoretically, the resolution of the water and oil flow measurement can be estimated to be 0.005 m/s, and 0.002 m/s respectively, at the pump power of 60% (~1.43 W). In terms of this specific performance, the sensor's performance is better than or at least comparable with the flow sensors reviewed in [14] regardless of the measurement of gas or fluids.

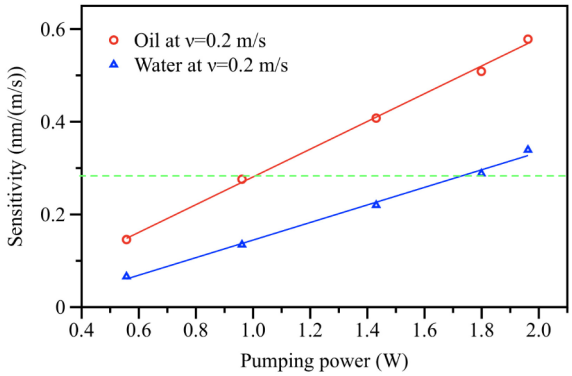


Fig. 8. Comparison of sensitivities as a function of pumping power for the oil and water flowing at the same speed of 0.2 m/s.

### *3.3 Real time measurement of the flow*

The oil flow measurement was also carried on in real time by changing the flow rate in steps from 0.516 m/s to 0.032 m/s. The hydraulic oil was used to monitor the flow measurement in real time and the pump power is set to be 60% (i.e. 1.43W). From the calibration results shown in Fig. 7(c), the Eq. (3) used to fit the measured data is: $\lambda = 1549.7 + 1.2089/(1.011 + 11.551v^{0.5})$. The flow rates measured using the FBG-based flowmeter were obtained using this equation and the measured Bragg wavelength. When the flow rate was adjusted, the Bragg wavelength was logged at the same time. Figure 9(a) shows the trace of the wavelength shift when the flow rate was reduced. It can be seen that when the flow rate stabilized at each step, the wavelength position remains unchanged. It takes some time for the flow rate to stabilize. Particularly, longer time is needed to stabilize lower flow rate. Figure 9(b) plots the comparison curves of flow rates measured by the FBG and the commercial flowmeter installed inside the flow controlling system of the test rig. The blue curve is the flow rates obtained by the FBG-based flowmeter and aforementioned equation, while the red curve is those measured by commercial flowmeter directly. The immediately after each flow rate reduction, dip was observed before it reached a stable value. These dips are due to the response time of the controlling system. This effect is more obvious for the cases with higher flow rate reduction. Consequently, the measured wavelength in real time also shows overshoot peaks, which represents the flow change at the same time. From the results, we can clearly see that the slight variation of the flow rate can be monitored by the sensor. Furthermore, the correlation coefficient of the flow rates measured by FBG and commercial flowmeter is calculated to be 0.9974, meaning that the flow sensor based on heated-FBG is comparable to the commercial flowmeter in terms of the accuracy. Note that there is a minor deviation (with a relatively error of ~5%) of the flow rates measured by the FBG-based flowmeter and commercial flowmeter, especially in the regime of high rates. This is probably

Optics EXPRESS

because of the lower sensitivity obtained in high flow rate, as shown in Fig. 7(d), and the heat instability on the flow sensor caused by fast flow.

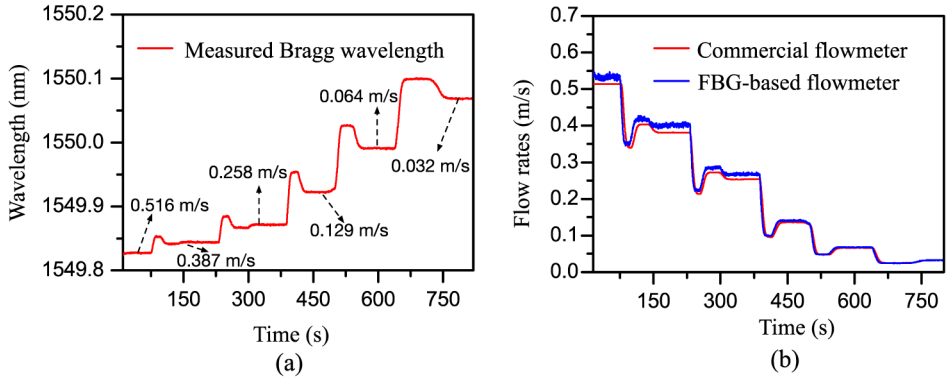


Fig. 9. (a) Bragg wavelength change monitored in real time when the flow rate is reduced step by step gradually, and (b) comparison curves of flow rates measured using heated-FBG flow sensor and a commercial flowmeter installed inside the test rig, both results have a correlation coefficient of 0.9974.

## 4. Conclusion

In this paper, we have demonstrated a miniature fluidic flow sensor based on FBG and $Co^{2+}$-doped fibers. The short FBG on a single mode fiber was heated by one or multiple $Co^{2+}$-doped multimode fibers. The $Co^{2+}$-doped multimode fibers convert the absorbed light energy to heat energy. The flow rates of water and hydraulic oil measured at different laser powers were measured based on the principle of hot-wire anemometer. The sensitivity obtained at $v$ = 0.2 m/s is 0.339 nm/(m/s) and 0.578 nm/(m/s) for water flow and oil flow, respectively, at the laser power of ~1.96 W. The high light-to-heat conversion efficiency of the $Co^{2+}$-doped multimode fibers allows high temperature difference to be created between the sensor head and fluids. Experimental results show that the sensitivity of the sensor can be further increased with higher laser power. The flow rates measured by the proposed flow sensor show a high correlation coefficient of 0.9974 with the commercial flowmeter, indicating its good performance. By monitoring the wavelength shift of the FBG, slight variation in flow rate can be distinguished.

The proposed miniature flow sensor measured flow rate ranging from 0~1 m/s using a standard interrogator. The sensor can measure the fluidic volume speed up to 30 L/min limited by the test rig, and can be potentially extended, which makes the flow sensor more feasible and attractive in oil industry. The resolution of the flow sensor is estimated to be 0.005 m/s and 0.002 m/s in measuring water and oil flow respectively, at the laser power of ~1.43 W, which is better than most electrical flow sensors reviewed in [14], and even FBG-based anemometer [5]. The capability of multiple pumping scheme can enable the extreme monitoring of hot oil. Owing to the features of compact size, immunity of electromagnetism, and free of electronics, the proposed miniature fiber optic flow sensor could be used in down-hole applications.

## Funding

The authors would like to acknowledge funding support from the Hong Kong RGC GRF under Grant PolyU5246/13E.